Experimental Observation of the Tellurium(IV) Bonding and Lone-Pair Electron Density in Dimethyltellurium Dichloride by X-ray Diffraction Techniques

Ronald F. Ziolo*[1a] and Jan M. Troup*[1b]

Contribution from Xerox Corporation, Webster Research Center, Webster, New York 14580, and Molecular Structure Corporation, College Station, Texas 77840. *Received August 11, 1981*

Abstract: The first detailed experimental electron deformation density of a heavy-atom molecule, dimethyltellurium dichloride, has been determined from high-resolution X-ray intensity measurements obtained at 151 K. A full sphere of 16 169 reflections was collected from a single crystal of the compound to a resolution of $(\sin\theta)/\lambda = 0.90$ using monochromatized Mo Kα radiation. After data reduction and absorption correction, a unique quadrant of 3937 reflections was created by averaging symmetry-related reflections. The internal agreement factor between equivalent observed reflections was 1.9% on F_o and 2.6% on I. A total of 3293 reflections having $I > 3\sigma(I)$ were considered to be observed. Full-matrix least-squares refinement including H atoms gave R (on F) = 0.0158 and R_w (on F) = 0.0224. The high-angle refinement used to minimize the effects of bonding and lone-pair electrons was accomplished with 863 reflections in the range $0.800 < (\sin\theta)/\lambda < 0.904$ Å^{-1}. Deformation density maps were calculated by using low-angle (<0.4 Å^{-1}) data. The 151 K structure is identical with the room-temperature structure reported by Christofferson, Sparks, and McCullough.[2] Deformation density maps clearly reveal Te(IV) bonding and lone-pair density consistent with classical bonding model predictions for AB_4E compounds. The asymmetric tellurium(IV) lone-pair density is predominantly localized and occupies the third equatorial site of the distorted pseudo trigonal bipyramid. The electron density in the elongated axial Te–Cl bonds is polarized toward Cl and has a distribution consistent with the interpretation that the covalent radius of the central atom in a tbp molecule is expanded in the axial direction. A trans arrangement of electron density is found in the C–Te···Cl2 segments of the crystal and is taken as evidence for the existence of intermolecular bonding in $(CH_3)_2TeCl_2$. The distribution supports a donor–acceptor model for the bonding that involves donation of the chlorine lone-pair density to an empty tellurium orbital. These observations provide direct experimental evidence in support of Alcock's thesis on secondary bonding to nonmetallic elements.[28] Deviations in the C–Te···Cl2 angles from linearity and perturbations in the solid-state molecular geometry are shown to be a consequence of the intermolecular bonding in combination with the equilibrium packing configuration of the molecules. The distribution of asymmetric lone-pair density about the bridging Cl2 suggests an approximate sp^2 hybridization for the bonding orbitals and a nonbonding, presumably p, orbital perpendicular to the plane of hybridization. Chlorine 1 is in a nonbonded environment and has a polarized asymmetric lone-pair distribution influenced by the electrostatic nature of the neighboring groups. A similar electrostatic influence is seen in the nonbonded lone-pair distributions about Te and Cl2. The difference in the electron distributions for the chlorine atoms demonstrates the effect of both weakly bonding and nonbonding intermolecular forces on the charge density distribution in $(CH_3)_2TeCl_2$.

Dimethyltellurium dichloride is a white crystalline solid containing tellurium in the hypervalent +4 formal oxidation state. The molecule is of the $AB_2B'_2E$ type and has a distorted pseudo-trigonal-bipyramidal (pseudo–tbp) geometry as demonstrated by Christofferson, Sparks, and McCullough.[2] The third equatorial site of the molecule presumably contains the tellurium(IV) lone pair. Although lone-pair and bonding electron densities have been observed directly in many materials by diffraction techniques,[3] no direct observation of the tellurium(IV) lone-pair or bonding density has been reported. To date, experimental electron density analyses have been confined mainly to compounds and materials containing atoms not heavier than the first transition series elements.[4]

As part of a larger effort to investigate the sterochemistry and bonding in hypervalent tellurium compounds, as well as the intermolecular bonding so prevalent in these compounds,[7] we have carried out an experimental electron deformation density study of the title compound by extension of the X–X deformation density technique.[8] This is the first such study reported for a molecule with trigonal-bipyramidal geometry.

Table I. Crystal Data for $(CH_3)_2TeCl_2$ (151 K)

space group	$P2_1/c$
a, Å	9.481 (4)
b, Å	6.115 (1)
c, Å	11.145 (3)
β, deg	98.14 (3)
V, Å^3	639.6
Z	4
D_{calcd} g/cm^3	2.373

Experimental Section

Dimethyltellurium dichloride was obtained from Organometallics, Inc., East Hampstead, NH 03826. High-quality crystals for X-ray diffraction were obtained by slow crystallization from 95% ethanol.

Collection of X-ray Data. An equidimensional colorless cube-shaped crystal measuring 0.21 × 0.25 × 0.25 mm was mounted on a thin glass fiber. Data were collected on an Enraf-Nonius CAD4 realtime diffractometer. An ultrastable dry-air refrigeration system low-temperature device constructed at Molecular Structure Corp. was used to cool the crystal to 151 ± 1 K for the attainment of accurate unit cell dimensions and reflection data. Mo Kα radiation (λ (Mo Kα) = 0.71073) was used

(1) (a) Xerox Corporation, Webster. (b) Molecular Structure Corporation, College Station.

(2) Christofferson, G. D.; Sparks, R. A.; McCullough, J. D. *Acta Crystallogr.* **1958**, *11*, 782.

(3) See, for instance: Coppens, P., Hall, M. B., Eds. "Electron Distributions and the Chemical Bond"; Plenum Press: New York, 1982. Becker, P., Ed. "Electron and Magnetization Densities in Molecules and Crystals"; Plenum Press: New York, 1980. Dunitz, J. D. "X-ray Analysis and the Structure of Organic Molecules"; Cornell University Press: Ithaca, NY, 1979; Chapter 8. Hirshfeld, F. L. *Isr. J. Chem.* **1977**, *16*, 87–229. Coppens, P.; Stevens, E. D. *Adv. Quantum Chem.* **1977**, *10*, 1–35. Coppens, P. *Int. Rev. Sci.; Inorg. Chem., Ser. Two* **1975**, *11*, 21–56. For a discussion of charge density distributions, see: Stewart, R. F.; Spackman, M. A. In "Structure and Bonding in Crystals"; O'Keeffe, M., Navrotsky, A., Eds.; Academic Press: New York, 1981; Vol. I, Chapter 12.

(4) Recently, some work involving molybdenum has appeared.[5,6]

(5) Troup, J. M.; Extine, M.; Ziolo, R. F. In "Electron Distributions and the Chemical Bond"; Coppens, P., Hall, M. B., Eds.; Plenum Press: New York, 1982; pp 285–296.

(6) Hino, K.; Saito, Y.; Benard, M. *Acta Crystallogr., Sect. B* **1981**, *B73*, 2164.

(7) Ziolo, R. F.; Titus, D. D. In "Proceedings of the 3rd International Symposium on Organic Selenium and Tellurium Chemistry"; Cagniant, D., Kirsch, G., Eds.; Universite de Metz: Metz, France, 1979; pp 319–347.

(8) Presented in part at the Symposium on Electron Distributions and the Chemical Bond, 181st National Meeting of the American Chemical Society, Atlanta, GA, March 29–April 3, 1981; American Chemical Society: Washington, D.C., 1981; INOR 52.

0002-7863/83/1505-0229$01.50/0

Table II. Positional and Thermal Parameters and Their Estimated Standard Deviations

atom		x	y	z	β_{11}[a] or B	β_{22}	β_{33}	β_{12}	β_{13}	β_{23}
Te	b	0.32348 (1)	0.11429 (1)	−0.16492 (1)	0.00414 (1)	0.01319 (2)	0.00297 (0)	−0.00052 (2)	0.00079 (1)	−0.00052 (1)
	c	0.32345 (2)	0.11434 (3)	−0.16495 (1)	0.00403 (1)	0.01294 (2)	0.00291 (1)	−0.00049 (4)	0.00074 (1)	0.00048 (3)
Cl1		0.14239 (5)	0.40745 (6)	−0.21343 (4)	0.00781 (4)	0.01430 (8)	0.00787 (3)	0.00354 (9)	−0.00002 (6)	0.00356 (8)
		0.1420 (1)	0.4077 (2)	−0.2140 (2)	0.00763 (7)	0.0138 (2)	0.00773 (8)	0.0032 (2)	−0.00012 (13)	0.0028 (2)
Cl2		0.48083 (4)	−0.21982 (7)	−0.11721 (3)	0.00766 (3)	0.02378 (9)	0.00503 (2)	0.01211 (9)	0.00006 (5)	−0.00429 (8)
		0.4809 (1)	−0.2199 (2)	−0.1168 (1)	0.00734 (2)	0.0234 (2)	0.00492 (4)	0.0118 (2)	−0.00030 (9)	−0.0047 (2)
C1		0.2401 (2)	−0.0473 (3)	−0.3275 (1)	0.0071 (1)	0.0173 (3)	0.00354 (7)	−0.0053 (4)	0.0006 (2)	−0.0018 (3)
		0.2400 (4)	−0.0474 (7)	−0.3275 (3)	0.0070 (2)	0.0162 (5)	0.0035 (1)	−0.0049 (6)	0.0009 (3)	−0.0015 (4)
C2		0.1849 (2)	−0.0294 (3)	−0.0549 (1)	0.0072 (1)	0.0170 (3)	0.00438 (8)	0.0006 (4)	0.0042 (2)	0.0024 (3)
		0.1844 (4)	−0.0298 (7)	−0.0546 (3)	0.0072 (2)	0.0169 (7)	0.0040 (1)	0.0014 (6)	0.0040 (2)	0.0025 (5)
H1	b	0.170 (2)	0.048 (5)	−0.361 (2)	4.5 (6)					
H2		0.312 (4)	−0.028 (7)	−0.390 (3)	10.2 (10)					
H3		0.207 (3)	−0.172 (5)	−0.311 (3)	6.3 (7)					
H4		0.091 (3)	0.030 (4)	−0.079 (2)	4.9 (6)					
H5		0.192 (3)	−0.164 (4)	−0.069 (2)	4.5 (6)					
H6		0.218 (3)	0.018 (4)	0.027 (2)	5.1 (6)					

[a] The form of the anisotropic thermal parameter is $\exp[-(h^2\beta_{11} + k^2\beta_{22} + l^2\beta_{33} + hk\beta_{12} + hl\beta_{13} + kl\beta_{23})]$. [b] Full-angle data refinement. [c] Refinement with $(\sin\theta)/\lambda \geq 0.800$.

with a graphite incident beam monochrometer. The diffractometer was set with a takeoff angle of 2.8°, an incident beam collimator diameter of 0.7 mm, and a counter aperture of 2.0 mm. The crystal to detector distance was 21 cm. Cell data for the crystal are given in Table I.

Reflection data were collected by using the θ–2θ scan technique with a variable scan rate ranging from 40°/min in 2θ for strong reflections to 4°/min in 2θ for weaker reflections. The angular scan range was from 0.6° before 2θ (Mo Kα^1) to 0.6° after 2θ (Mo Kα^2) with the ratio of scan time to background counting time at 2:1. A full sphere or 16 169 reflections were scanned to a 2θ (Mo Kα)$_{max}$ = 80°. Three representative reflections were checked periodically for crystal and electronic stability and were found to show no significant change. The data were corrected for Lorentz and polarization factors and for absorption (μ = 54.97 cm^{-1}). The programs used in the data reduction and in the solution and refinement of the structure were part of the Enraf-Nonius Structure Determination Package.[9] Four Ψ scans at various 2θ values were measured through a full 360°. No evidence for a 2θ dependence at different 2θ values was observed. The average of the four Ψ scans used for the absorption correction showed a maximum correction of 11.6% in F_o and the average correction was 4.3% in F_o. A unique quadrant of 3937 data was created by using an averaging program where $I_{ave} = (\sum^n I_i)/n$ and $\sigma I = [\sum^n \sigma(I_i)]/n$. The worst of the averaged reflections was rejected when $[I_o - I_{ave}] > 5\sigma(I_o)$, providing at least two good reflections remained. The internal agreement factor between equivalent observed reflections was 1.9% on F_o and 2.6% on I. The agreement factor is excellent in view of the large number of data collected, the temperature of the data collection, and the necessity of an absorption correction. A total of 3293 averaged reflections had intensities with $I > 3\sigma I$ and were considered to be observed. Here, $I = S(C - RB)$ and $\sigma(I) = [S^2(C + R^2B) + p(I)^2]^{1/2}$, where S = scan rate, C = total integrated peak count, R = ratio of scan time to background counting time, B = total background count, and p = 0.02.

Solution and Refinement. At the onset of the structure refinement the positional parameters from the room-temperature study[2] were not immediately available so the structure was solved for all non-hydrogen atoms by direct methods with the program MULTAN. Following several cycles of full-matrix least-squares refinement, the hydrogen atoms were located in a difference Fourier map. The structure was refined anisotropically for non-hydrogen atoms and isotropically for hydrogen atoms to convergence by using all of the unique observed data. The resulting agreement factors were R_1 = 0.0158 and R_2 = 0.0224 where $R_1 = \sum||F_o| - |F_c||/\sum|F_o|$ and $R_2 = [\sum w(|F_o| - |F_c|)^2/\sum wF_o^2]^{1/2}$. In the full-matrix least-squares refinement the function minized was $\sum w(|F_o| - |F_c|)^2$ where the weight w is defined as $4F_o^2/\sigma^2(F_o^2)$. Atomic scattering factors were from the compilation of Cromer and Waber[10] and were corrected for anomalous dispersion in both the real and imaginary parts.[11] In the final cycle of refinement, the maximum parameter shift was 0.02 times its esd, and the esd of an observation of unit weight was 1.19. The agreement factor including unobserved data was 0.0211. Isotropic extinction was refined and was found to be small, converging to 7.198 × 10^{-7}. The final data to parameter ratio for the full data refinement was 46.4:1, and the $(\sin\theta/\lambda)_{max}$ was 0.904 Å^{-1}. Plots of the average $w(|F_o| - |F_o|)^2$ vs. $|F_o|$, reflection order, and various classes of indicies showed no unusual trends.

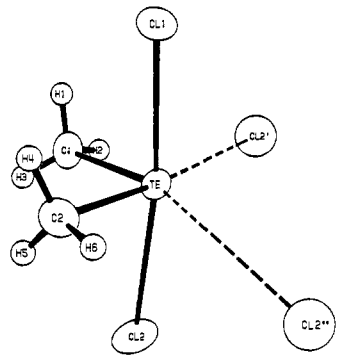

Figure 1. ORTEP drawing of $(CH_3)_2TeCl_2$ showing ellipsoids of 50% probability and the atom labeling scheme. Hydrogen atoms were given arbitrary radii for clarity.

The atomic coordinates and anisotropic thermal parameters for both the full data refinement and the high-angle data refinement are given in Table II. The values of the B and U parameters with their esd's are given in Table III. Tables of the root-mean-square amplitudes of thermal vibration and observed and calculated structure factors for both the observed and unobserved data are given as supplementary material.

Results and Discussion

Structural Results at 151 K. Bond distances and angles from the full and high-angle data refinements are reported in Table IV and agree to within two estimated standard deviations of the room-temperature values determined from film data.[2] An ORTEP drawing of the molecule with its secondary contacts and atom labeling scheme is presented in Figure 1 and a stereoscopic unit-cell view is given in Figure 2.

Calculation of Deformation Density. The calculation of deformation density was performed by subtracting the A and B terms calculated from high-order parameters and phases, which would approximate spherical atoms, from the observed structure factors,[12] i.e.:

$$\Delta\rho = (2/V)(\sum_h\sum_k\sum_l[(A_{obsd}/k) - A_{calcd}](\cos 2\pi) \times (hx + ky + lz) + [(B_{obsd}/k) - B_{calcd}](\sin 2\pi)(hx + ky + lz))$$

where k is the scale factor for the high-order refinement. The high-angle refinement used to minimize the effects of bonding and lone-pair electrons was accomplished with 863 reflections in the range of $0.800 < (\sin\theta)/\lambda < 0.904$ Å^{-1}. Hydrogen atom positions were included as a constant contribution in the high-angle refinement. Both full data and low-angle ($(\sin\theta)/\lambda < 0.4$ Å^{-1}) data deformation density maps were prepared. The maps cal-

(9) Enraf-Nonius Structure Determination Package (SDP), Enraf-Nonius, Delft, Holland, revised 1979 by B. A. Frenz.

(10) Cromer, D. T.; Waber, J. T. "International Tables for X-ray Crystallography"; Kynoch Press: Birmingham, England, 1974; Vol. IV, Table 2.2B.

(11) Cromer, D. T.; Liberman, D. *J. Chem. Phys.* **1970**, *53*, 1891.

(12) Coppens, P. *Acta Crystallogr., Sect. B* **1974**, *B30*, 255.

Table III. General Temperature Factor Expressions

atom		B_{11}	B_{22}	B_{33}	B_{12}	B_{13}	B_{23}
Te	*a*	1.460 (3)	1.972 (3)	1.447 (2)	−0.060 (2)	0.164 (2)	−0.070 (2)
	b	1.420 (2)	1.935 (3)	1.417 (2)	−0.056 (4)	0.152 (2)	−0.065 (4)
Cl1		2.75 (1)	2.14 (1)	3.83 (2)	0.41 (1)	−0.00 (1)	0.48 (1)
		2.69 (3)	2.07 (2)	3.76 (4)	0.37 (2)	−0.02 (3)	0.38 (2)
Cl2		2.70 (1)	3.56 (1)	2.45 (1)	1.39 (1)	0.01 (1)	−0.58 (1)
		2.59 (2)	3.49 (3)	2.39 (2)	1.35 (2)	−0.06 (2)	−0.63 (2)
C1		2.49 (4)	2.59 (4)	1.72 (4)	−0.61 (4)	0.12 (3)	−0.24 (4)
		2.48 (8)	2.42 (8)	1.70 (5)	−0.57 (7)	0.19 (6)	−0.21 (6)
C2		2.52 (4)	2.54 (5)	2.13 (4)	0.07 (4)	0.88 (3)	0.33 (4)
		2.55 (7)	2.5 (1)	1.95 (6)	0.16 (7)	0.83 (5)	0.33 (6)
atom		U_{11}	U_{22}	U_{33}	U_{12}	U_{13}	U_{23}
Te	*a*	0.01849 (3)	0.02498 (3)	0.01833 (3)	−0.00076 (3)	0.00207 (2)	−0.00088 (2)
	b	0.01799 (3)	0.02451 (4)	0.01795 (3)	−0.00071 (5)	0.00193 (3)	−0.00082 (6)
Cl1		0.0348 (2)	0.0271 (1)	0.0485 (2)	0.0052 (1)	−0.0001 (2)	0.0061 (1)
		0.0341 (3)	0.0262 (3)	0.0477 (5)	0.0047 (3)	−0.0003 (3)	0.0049 (3)
Cl2		0.0342 (1)	0.0451 (2)	0.0310 (1)	0.0176 (1)	0.0002 (1)	−0.0073 (1)
		0.0328 (3)	0.0443 (4)	0.0303 (3)	0.0171 (2)	−0.0008 (2)	−0.0080 (3)
C1		0.0315 (6)	0.0328 (6)	0.0218 (5)	−0.0078 (5)	0.0015 (4)	−0.0030 (5)
		0.031 (1)	0.031 (1)	0.0215 (7)	−0.0072 (9)	0.0024 (7)	−0.0026 (8)
C2		0.0319 (5)	0.0322 (6)	0.0270 (5)	0.0009 (5)	0.0111 (4)	0.0041 (5)
		0.0323 (9)	0.032 (1)	0.0247 (7)	0.0020 (9)	0.0105 (7)	0.0042 (8)

[a] Full-angle data refinement. [b] Refinement with $(\sin\theta)/\lambda \geq 0.8$ Å^{-1}.

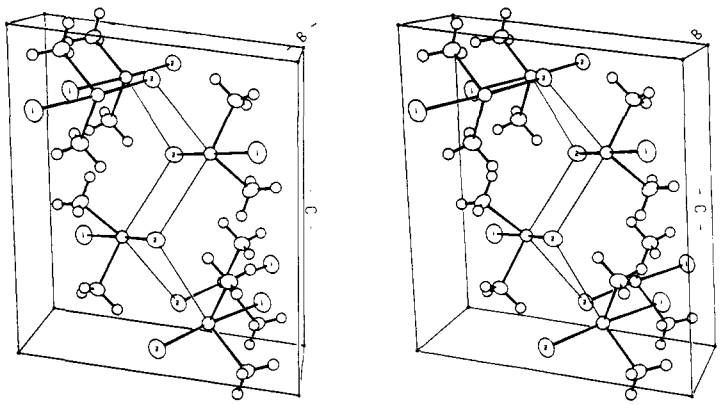

Figure 2. Stereoscopic unit-cell view of $(CH_3)_2TeCl_2$.

culated from the full set of unique data were noisy and did not show clearly the bonding electron density. Although exceptionally good quality, high-resolution data should be beneficial in such determinations, inclusion of data far beyond the scattering ability of the bonding and lone-pair densities appears only to increase random errors. When maps were calculated from low-angle data by using a $(\sin\theta)/\lambda$ cutoff, reasonable bonding and lone-pair electron densities were clearly revealed. In the present case, a $(\sin\theta)/\lambda < 0.40$ Å^{-1} cutoff was found to be a good compromise between resolution and map clarity. Lower $(\sin\theta)/\lambda$ cutoffs showed a definite loss of resolution with little noise reduction, while higher cutoffs gave less well-defined bonding density. We have successfully invoked this compromise between increasing resolution and the frequency of random errors in other heavy-atom studies where small changes in electron sphericity about the heavy-atom core were examined in the calculations of the deformation density.[5]

Electron deformation maps were calculated for numerous planes in the structure including the equatorial plane and the axial plane containing Te, Cl1, and Cl2. Since the magnitude of the peaks in an electron density map depends on the number of terms in the structure factor calculation, the $(\sin\theta)/\lambda$ cutoff gave reduced peak heights when compared to values obtained from full data maps. Therefore, as an internal standard to help quantify the electron density, H6 was removed from the structure factor calculation and a deformation map was prepared. The peak-height value of H6 was found to be 0.54 e/Å^3 as compared to 0.27 e/Å^3 for the tellurium lone pair.

An evaluation of the error in an electron density map not near atomic positions was given by Cruickshank[13] as $\sigma^2F_o = 2/V^2\sum_{n=0}\sigma^2(F)$. The Cruickshank expression is a good estimate of the average map error and is that given in Figures 3 through 6. Near atomic positions, contributions to the error from the uncertainty in the scale factor,[14] and atomic positional[15] and thermal parameters[16] increase rapidly.[17] The error due to uncertainty in thermal parameters is probably the most difficult to estimate and has been evaluated by Stewart[16] to be small at a distance of 0.4 Å from atomic positions. In the present study, density within approximately 0.4 Å of the atomic center should be considered as having a high error. No major feature of electron density relevant to our discussion, however, is present within this area.

Discussion of Deformation Density. The deformation density in the equatorial and axial planes in $(CH_3)_2TeCl_2$ is shown in Figures 3 and 4, respectively. Distinct electron density peaks are observed in the tellurium–carbon, tellurium–chlorine, and carbon–hydrogen bonds.[18] The density distribution is nonspherical as is usually found in σ-bonded interactions.[19] The most prominant feature in the maps is the single peak of 0.27 e/Å^3 located approximately 0.9 Å from Te in the third equatorial site of the pseudo trigonal bipyramid. This density is attributed to the

(13) Cruickshank, D. W. J. *Acta Crystallogr.* **1949**, *2*, 65.
(14) Rees, B. *Acta Crystallogr., Sect. A* **1978**, *A34*, 254.
(15) Dawson, B. *Acta Crystallogr.* **1964**, *17*, 990.
(16) Stewart, R. F. *Acta Crystallogr., Sect. A* **1968**, *A24*, 497.
(17) Stevens, E. D.; Coppens, P. *Acta Crystallogr., Sect. A* **1976**, *A32*, 915.
(18) Deformation density maps calculated for planes parallel to and ±0.75 Å away from the equatorial plane indicate a small amount of static disorder (staggered configuration) in the methyl group positions.
(19) See, for instance: Coppens and Stevens, and Coppens, ref 3.

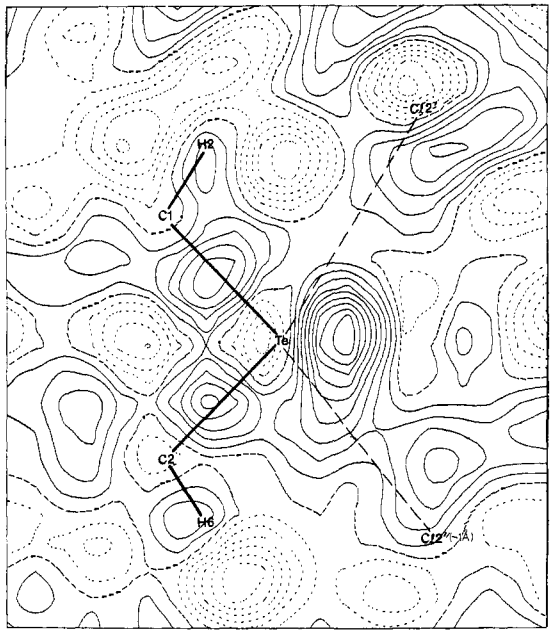

Figure 3. Deformation density map for $(CH_3)_2TeCl_2$ in the equatorial Te, C1, C2 plane showing the Te–C bond and Te(IV) lone-pair densities. Contours are at 0.03 e/Å^3 with negative contours broken. The error in density is 0.03 e/Å^3. Atoms H2, H6, and one symmetry related Cl2 are also in the plane; a second symmetry related Cl2 is 1 Å below the plane.

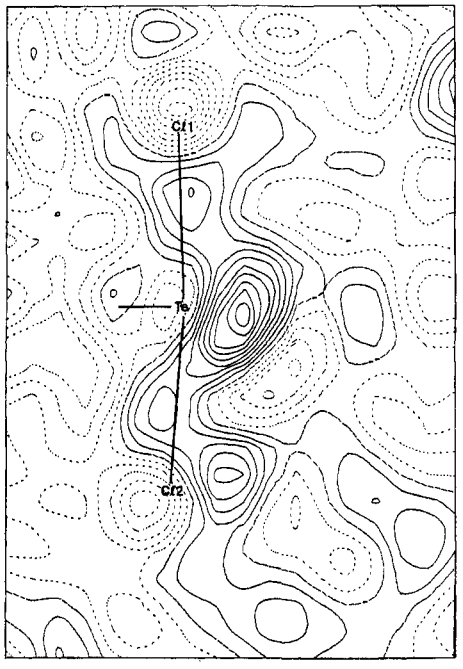

Figure 4. Deformation density map for $(CH_3)_2TeCl_2$ perpendicular to the plane in Figure 3 showing the Te–Cl bond and Te(IV) lone-pair densities. Atoms Te, Cl1, Cl2 and the bisector of the C1–Te–C2 angle are in the plane. Contours and errors are as in Figure 3.

tellurium(IV) "nonbonded" or "lone" pair and occupies the site generally presumed to be the lone-pair region in trigonal-bipyramidal AB_4E molecules.[20] The observed electron density distribution is taken as evidence that the nonspherical part of the tellurium(IV) lone-pair density[21] in $(CH_3)_2TeCl_2$ is significantly localized and that it occupies an equatorial position in the molecule. Figure 4 and sections above and below the equatorial plane show a significant shift in the centroid of the lone-pair density out of the equatorial plane toward Cl2 (vide infra). We note that the deformation density about tellurium is consistent with the valence-shell electron-pair repulsion (VSEPR) model rule that lone-pair electrons take up more room on the surface of an atom than the bonding pairs.[22]

A salient feature of the trigonal-bipyramidal molecules is the elongation of their axial bonds. Typically, the elongation is about 0.1–0.2 Å greater than the normal covalent distance, to give an interaction having a bond order[23a] of 0.5. In $(CH_3)_2TeCl_2$, the axial distances are 0.13 and 0.18 Å longer than the sum of the normal covalent radii, 2.36 Å.[23b] Figure 4 shows the deformation density in the axial plane containing Te, Cl1, Cl2, and the bisector of the C–Te–C angle. Distinct electron density peaks are observed between the tellurium and chlorine atoms, consistent with the expected covalent nature of the axial Te–Cl bond. The centroids of the Te–Cl density occur approximately 1 Å from the chlorine nuclei, at a distance corresponding to the normal covalent radius of chlorine. Thus, the electron density is significantly displaced from the bond midpoint toward chlorine in agreement with the interpretation that the covalent radius of the central atom in a trigonal-bipyramidal molecule is greater in the axial than in the

Table IV. Interatomic Distances (Å) and Angles (deg)[a]

atoms[b]	full data refinement	refinement with $(\sin\theta)/\lambda \geq 0.8$ Å^{-1}
Te–Cl1	2.488 (1)	2.492 (1)
Te–Cl2	2.541 (1)	2.543 (1)
Te–Cl2′	3.412 (1)	3.415 (1)
Te–Cl2″	3.478 (1)	3.474 (1)
Te–C1	2.116 (1)	2.117 (4)
Te–C2	2.112 (1)	2.118 (4)
C1–H1	0.92 (3)	
C1–H2	1.04 (4)	
C1–H3	0.85 (3)	
C2–H4	0.97 (3)	
C2–H5	0.84 (3)	
C2–H6	0.97 (3)	
Cl1–Te–Cl2	172.44 (1)	172.40 (6)
Cl1–Te–Cl2′	93.39 (1)	93.31 (6)
Cl1–Te–Cl2″	109.04 (1)	109.17 (5)
Cl1–Te–C1	89.29 (5)	89.18 (16)
Cl1–Te–C2	87.66 (4)	87.71 (14)
Cl2–Te–Cl2′	91.47 (1)	91.55 (3)
Cl2–Te–Cl2″	74.80 (1)	74.70 (5)
Cl2–Te–C1	86.61 (5)	86.69 (15)
Cl2–Te–C2	86.50 (4)	86.44 (14)
Cl2′–Te–Cl2″	108.30 (1)	108.31 (4)
Cl2′–Te–C1	72.80 (4)	72.78 (11)
Cl2′–Te–C2	169.35 (4)	169.29 (14)
Cl2″–Te–C1	161.37 (5)	161.35 (15)
Cl2″–Te–C2	81.27 (4)	81.32 (14)
C1–Te–C2	96.63 (6)	96.59 (18)
Te–Cl2′–Te′	116.89 (1)	
Te–Cl2′–Te″	115.09 (1)	
Te′–Cl2′–Te″	105.22 (1)	
Te–C1–H1	102.0 (2)	
Te–C1–H2	108.0 (2)	
Te–C1–H3	110.0 (2)	
H1–C1–H2	100.0 (3)	
H1–C1–H3	113.0 (3)	
H2–C1–H3	122.0 (3)	
Te–C2–H4	108.0 (2)	
Te–C2–H5	103.0 (2)	
Te–C2–H6	106.0 (2)	
H4–C2–H5	114.0 (2)	
H4–C2–H6	108.0 (2)	
H5–C2–H6	116.0 (2)	

[a] Numbers in parentheses are estimated standard deviations in the least significant digits. [b] Single primed atoms at $[1-x, {}^1/_2 + y, -{}^1/_2 - z]$; doubly primed atoms at $[1-x, \bar{y}, \bar{z}]$.

(20) See, for instance: Gillespie, R. J. "Molecular Geometry"; Van Nostrand Reinhold: New York, 1972.
(21) The observed lone-pair density is that part which is in excess of any spherical atomic distribution.
(22) Gillespie, R. J. *J. Chem. Ed.* **1970**, *47*, 18–23.
(23) Pauling, L. "The Nature of the Chemical Bond", 3rd ed.; Cornell University Press: Ithaca, NY, 1960; (a) p 255, (b) p 224.

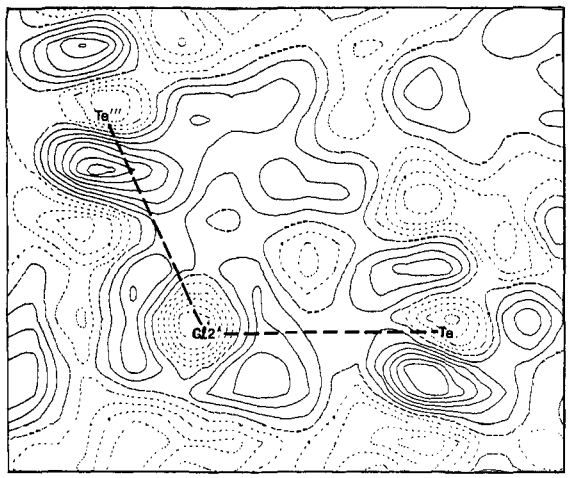

Figure 5. Deformation density map for $(CH_3)_2TeCl_2$ in the Te–Cl2′–Te‴ plane showing the distribution of the Cl2 lone-pair density along the Te···Cl directions. Contours and errors are as in Figure 3; tellurium triple prime is at x, $1/2 - y$, $-1/2 + z$.

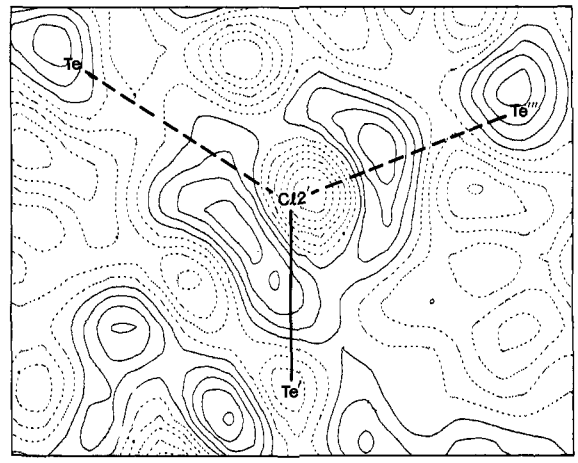

Figure 6. Deformation density map calculated in the plane containing Cl2′ and located 1.06, 0.43, and 1.20 Å below Te, Te′, and Te‴, respectively. Contours and errors are as in Figure 3.

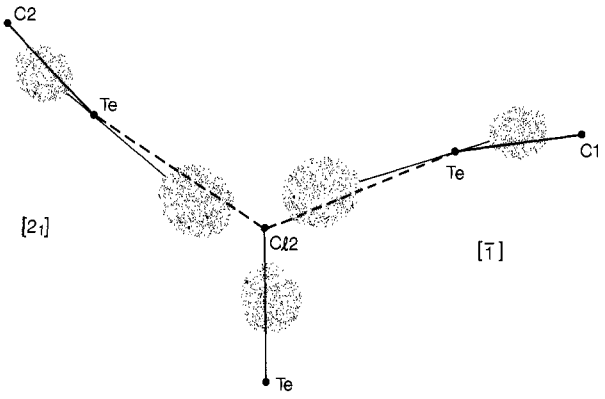

Figure 7. Proposed intermolecular bonding scheme in $(CH_3)_2TeCl_2$ utilizing an sp^2 hybridization for the bonding orbitals of the bridging Cl2 and a donor–acceptor model for the Te···Cl2 interactions. A nonbonding Cl2 p orbital is normal to the plane. Molecules are related by an inversion center and a twofold screw axis parallel to b (Figure 2).

equatorial direction.[24] The elongation observed in tbp molecules has been explained in terms of various models.[20,24-26] A slight polarization of the Te–C bond density is also noted, although the displacement of the peak maxima from the bond midpoints is only marginally, if at all, significant. The polarization of electron density in heteronuclear bonds of normal covalent length has been noted previously.[19]

Of particular significance in solid dimethyltellurium dichloride are the short intermolecular Te···Cl2 contacts at 3.412 (1) and 3.478 (1) Å that give tellurium(IV) a six-coordinate distorted-octahedral geometry. It has been inferred from an abundance of crystal structure data[27,28] that such contacts constitute weak or secondary bonding between the participating atoms. Alcock[28] has proposed a donor–acceptor model for the interaction that involves electron density on the distal atom and an empty, presumably σ^* orbital on the central atom. Although very little is known about the nature of the forces in these interactions, recent structure determinations of $(C_6H_5)_3SeNCS$[29] and of the mono- and dihydrates of $(C_6H_5)_3SeCl$[30,31] strongly support the bonding model. Charge density studies of seconary bonding in compounds of the type considered by Alcock[28] have not appeared previously. In molecular chlorine, however, where intermolecular contacts considerably shorter than the van der Waals distance are observed, no indication of a bonding peak was found in the directions corresponding to the short intermolecular contacts.[32]

In the present case, the deformation density maps calculated around Cl2 reveal two regions of asymmetric lone-pair density concentrated in the directions of the two closest tellurium atoms from neighboring molecules.[33] Part of this density is revealed in the deformation density map (Figure 5) calculated in the Te, Cl2′, Te‴ (x, $^1/_2 - y$, $- ^1/_2 + z$) plane that contains the two intermolecular Te···Cl2 vectors. Here, the density regions are seen as two broad peaks with heights of 0.09e/Å^3 on each side of Cl2′ just off the Te···Cl2 internuclear axes. The most important feature of the two density regions is their stereochemically significant location trans to the Te–C bond density of the associated molecule. This relationship is seen in Figure 3 for both C–Te···Cl2 interactions where the C–Te and Cl2···Te densities reach their maximum value. With the exception of the C2–Te density, the maxima persist into the Te–Cl2′–Cl2″ plane as well. Within experimental error, the centroids of the two densities in the C–Te···Cl2 interactions subtend an angle of 180° about tellurium. The observed directionality of charge in combination with the short Te···Cl2 distances is taken as evidence for the existence of intermolecular bonding in $(CH_3)_2TeCl_2$ and strongly supports the donor–acceptor model for the bonding, involving donation of the chlorine lone-pair density to an empty orbital on tellurium.[34] These observations provide direct experimental evidence in support of Alcock's thesis on secondary bonding to nonmetallic elements[28] and an explantation, in terms of the charge density distribution, for the octahedral coordination about tellurium. As a consequence of the linear relationship of electron density, the positions of the centroids of the bond density about tellurium show significantly less distortion from octahedral geometry than the atomic positions.[35] The observed charge density is also consistent with the observation that no secondary bonds form in the direction of the central atom's lone pair.[29,30]

(24) Cotton, F. A.; Wilkinson, G. "Advanced Inorganic Chemistry", 4th ed.; Interscience: New York, 1980; Chapter 5.
(25) Gillespie, R. J. *Can. J. Chem.* **1961**, *39*, 318–323.
(26) Wynne, K. J. *Adv. Chem. Ser.* **1972**, *110*, 150.
(27) Zemann, J. *Monatsh. Chem.* **1971**, *102*, 1209.
(28) Alcock, N. W. *Adv. Inorg. Chem. Radiochem.* **1972**, *15*, 1.
(29) Ash, P. A.; Lee, J.-S.; Titus, D. D.; Mertes, K.; Ziolo, R. F. *J. Organomet. Chem.* **1977**, *135*, 91.
(30) Mitcham, R. V.; Lee, B.; Mertes, K.; Ziolo, R. F. *Inorg. Chem.* **1979**, *18*, 3498.
(31) Lee, J.-S.; Titus, D. D. *J. Cryst. Mol. Struct.* **1976**, *6*, 279.
(32) Stevens, E. D. *Mol. Phys.* **1979**, *37*, 27.
(33) A description of the molecular packing in $(CH_3)_2TeCl_2$ is given in ref 2. In the crystal, molecules pack to form two layers parallel to (100) that interact through the two short intermolecular Te···Cl2 contacts to form double-layered sheets with methyl groups and Cl1 atoms protruding on each side (Figure 2). Adjacent sheets pack forming pockets of methyl groups occupied by Cl1 atoms (Figure 8).
(34) An electrostatic description is also possible; see, for instance: Hirshfeld, F. L. In "Electron and Magnetization Densities in Molecules and Crystals"; Becker, P., Ed.; Plenum: New York, 1980; pp 47–62.
(35) Whether or not the small displacement of Te–C bond density off the internuclear axes to make an angle smaller than the 97° C1–Te–C2 angle is significant, must await further experimental study.

Relative to the crystal geometry, Cl2 is located at the apex of a distorted trigonal pyramid whose base comprises the three nearest-neighbor tellurium atoms as seen in Figure 2. The intermolecular Te–Cl2–Te angles (Table IV) range from 105 to 117°, and, together with the positions of the two electron density peaks noted above, suggest the possibility of an sp^2 or sp^3 hybridization for the bonding orbitals of Cl2. To examine these possibilities, we calculated a series of deformation density maps at 0.3-Å intervals in planes parallel to the base of the pyramid above, below, and through Cl2. The maps revealed no electron density in the direction of the fourth tetrahedral position, which is near a Cl1 $(x, y - 1, z)$ atom, 3.96 Å from Cl2. Although the electron density peaks are broad due to the larger thermal parameters for chlorine, an approximately trigonal arrangement of density about Cl2 involving the two secondary bond densities and the Te–Cl2 primary bond density is evident when the total density about Cl2 is examined. The general features of the deformation density near the maxima of the three densities is seen in Figure 6, which represents the deformation density map calculated in the plane containing Cl2′ and located 1.06, 0.43, and 1.20 Å below Te, Te′, and Te‴, respectively. Here, the Te′–Cl2′ and Te–Cl2′ densities occur as an elongated peak with two maxima.

Two additional peaks of Cl2 asymmetric lone-pair density are found above and below the plane in Figure 6, approximately on the pseudothreefold axis of the distorted trigonal pyramid. The more intense peak has a maximum intensity of 0.15e/Å^3 and may be seen to the right of Cl2 in Figure 4. The maximum is located in the three-atom plane of electropositive tellurium atoms approximately 0.8 Å from the Cl2 nucleus. The other peak which is below the plane in Figure 6 has a maximum intensity of 0.09e/Å^3 and is located just off the pseudothreefold axis of the trigonal pyramid on the other side of Cl2 above the plane in Figure 4. The direction of displacement of this density off the threefold axis is away from the nearby Cl1 atom at $(x, y - 1, z)$ and toward a neighboring methyl group on a molecule in the same sheet related by a $[2_1 + \bar{1}]$ operation. The general appearance of the asymmetric lone-pair density distribution about Cl2 is consistent with approximate sp^2 hybridization of the bonding orbitals (primary and secondary) and with a nonbonding, presumably p orbital perpendicular to the trigonal hybrid. A model for the intermolecular bonding in $(CH_3)_2TeCl2$ based on these observations is given in Figure 7. The diagram shows the essential parts of three molecules bridged by Cl2 and related by a 2_1 or $\bar{1}$ operation. The off-axis bonding, which is noted throughout the structure except in the case of the Te–Cl1 density, has been exaggerated to illustrate the linear relationship of the electron density in the C–Te···Cl2 segments and the C–Te···Cl2 angle. A similar bonding situation might be expected in α-$C_8H_8TeI_2$.[36]

As a consequence of the combination of the electronic requirements of the donor–acceptor interaction, the hybridization of the bonding orbitals of the briding chlorine atom and the equilibrium packing configuration of the molecules, the C–Te···Cl angles in the structure are observed to be nonlinear. Previous X-ray structural analyses of numerous compounds exhibiting secondary bonding have shown that deviations of up to 15° from linearity are common in the B–A···B′ angle.[28] In the present case, the significance of the nonlinearity of the C–Te···Cl2 angles is clearly revealed in the deformation density maps. In the original structure determination,[2] the difference between the Te–Cl bond lengths was noted and correctly attributed to the participation of Cl2 in the intermolecular bonding. Figure 4 shows an off-axis density in the Te–Cl2 bond, which is also taken to be a consequence of the combination of the above factors. Although the shift is of borderline significance, we note that it is in the correct direction to explain the increased length in the Te–Cl2 bond over

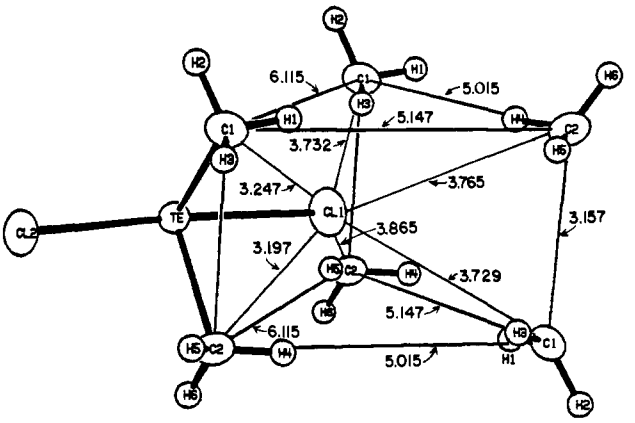

Figure 8. Nearest-neighbor methyl group environment about chlorine 1. Distances in Å.

that of the Te–Cl1 bond (53σ) and the slight shift of the tellurium asymmetric lone-pair density toward the Cl2 nucleus (or, alternatively, away from the Te–Cl1 density).[37] In the isolated molecule, the centroid of the tellurium lone-pair density would be expected to lie in the equatorial plane. Perturbations in the solid-state molecular geometry of the compound, such as the more acute C–Te–Cl2 angles and the Cl1–Te–Cl2 angle, also presumably relate, at least in part, to these factors. Although steric effects cannot be completely ruled out, the present data along with the recent structure determination of tetraphenyltellurium[38] strongly suggest the predominance of electronic effects over steric effects in determining the direction of bend in the axial B′–A–B′ angle.

A pronounced polarization of asymmetric lone-pair density is observed about Cl1, which, unlike Cl2, is in a nonbonded environment. This density, as determined from deformation density maps calculated at 0.3-Å intervals in planes parallel to the equatorial plane above, below, and through Cl1, is in the form of two lobes, each having roughly a "half-moon" shape and located above and below the axial plane in Figure 4. The lobes project toward the positive regions in the crystal formed by the nearest-neighbor methyl groups that are located at the vertices of a distorted trigonal prism illustrated in Figure 8.[39] One lobe has a maximum peak-height value of 0.21 e/Å^3 and projects downward in the figure to the rear. The other lobe, which is much more diffuse, has a peak density of 0.09e/Å^3 and is located approximately opposite the lower lobe, projecting upward and slightly forward in the drawing. The plane through Cl1 and parallel to the equatorial plane shows two additional peaks at 0.03 and 0.06 e/Å^3 at right angles to the larger peaks. Part of this density is visible as the wing-shaped feature of the Te–Cl1 density in Figure 4. These peaks lie very nearly in the direction of a neighboring Cl2 atom at $(x, 1 + y, z)$ and another Cl1 atom at $(1 - x, 1 - y, z)$. The extent to which the distribution approximates three mutually perpendicular p orbitals, or, alternatively, an sp hybrid and two p orbitals, cannot be assessed in the present experiment since little or no significance can be attahced to the low-intensity peaks or to the peak at 0.03 e/Å^3 above Cl1 in Figure 4. The observed polarization of density toward the positive regions in the crystal and the lack of density in the direction of negative regions in the crystal do, however, suggest substantial influence of the neighboring groups or atoms on the nonbonding density about Cl1. This situation is similar to that observed for the nonbonding density of Cl2 and to a lesser extent to that observed for tellurium (vide supra). Although these distributions are physically reasonable from an electrostatics point of view, their full significance must await the results of a higher resolution study of the compound and a better understanding of the field of electron density analyses in general. At present, the study of such effects is in its infancy and has so far been limited almost completely to hydrogen-bonded complexes.[40] In the present case, the difference observed between the electron distributions about the chlorine atoms clearly dem-

(36) Knobler, C.; Ziolo, R. F. *J. Organomet. Chem.* **1979**, *178*, 423.

(37) Although there is crystallographic evidence that suggests the possible involvement of the Te(IV) lone pair in the bonding in several compounds (see, for example, Buss, B.; Krebs, B. *Inorg. Chem.* **1971**, *12*, 2795), no significance can be attached to the overlap of density peaks observed in the deformation density maps at the present degree of resolution.

(38) Smith, C. S.; Lee, J.-S.; Titus, D. D.; Ziolo, R. F. *Organometallics* **1982**, *1*, 350.

(39) Two additional methyl groups are located at about 4 and 5 Å from Cl1 in the direction of each lobe.

onstrates the effect of both weakly bonding and nonbonding intermolecular forces on the charge density distribution in dimethyltellurium dichloride.

Summary and Conclusions

The first detailed experimental electron density study of a heavy-atom molecule, dimethyltellurium dichloride, has been carried out with sufficient resolution to reveal bonding and asymmetric lone-pair electron density by extension of the X-X deformation density technique. The following chemically significant features of the intramolecular and intermolecular bonding in the compound have been noted. (1) The bonding and lone-pair density in the molecule is consistent with the predictions of classical bonding models for AB_4E molecules. The asymmetric lone-pair density is predominantly localized and is found to occupy the third equatorial position of the distorted Ψ-trigonal-bipyramid. (2) The bonding density in the axial Te-Cl bonds of order 0.5 is polarized toward chlorine and has a distribution consistent with the interpretation that the covalent radius of the central atom in a tbp molecule is expanded in the axial direction. (3) The trans arrangement of electron density observed in the C-Te···Cl segments of the crystal suggests a donor-acceptor type interaction for the intermolecular bonding in $(CH_3)_2TeCl_2$. These observations provide direct experimental evidence in support of Alcock's thesis[28] on secondary bonding to nonmetallic elements. (4) The deviation of the C-Te···Cl angle from linearity and perturbations in the solid-state molecular geometry of $(CH_3)_2TeCl_2$ are a consequence of the intermolecular bonding in the compound in combination with the equilibrium packing configuration of the molecules. (5) The asymmetric lone-pair density distribution about Cl2 is consistent with an approximate sp^2 hybridization of the bonding orbitals and a nonbonding, presumably p orbital perpendicular to the trigonal hybrid. A pronounced polarization of asymmetric lone-pair density is observed about Cl1, which is in a nonbonded environment. (6) The influence of electrostatic forces of neighboring groups or atoms is evident in the distribution of nonbonding density about Cl1, Cl2, and Te. As in the case of bonding density, more charge is found directed toward the positive regions in the crystal than toward the negative regions in the crystal. (7) The difference between the chlorine atom electron distributions demonstrates the effect of both weakly bonding and nonbonding intermolecular forces on the charge density distribution in dimethyltellurium dichloride.

The observations made herein are consistent with the known structural data for tellurium(IV) compounds and with the results of recent electron density distribution studies on the distorted octahedral compounds, $(CH_3)_3TeCl$ and $(CH_3)_3TeBr$.[41] The full significance of the observations, however, must await further experimental studies with equal or higher resolution on other heavy-atom molecules, exploration of the sin θ/λ cutoff technique, a more accurate assessment of deformation density map errors, and the appearance of theoretical studies on molecules containing heavy-atom, main-group elements.

Acknowledgment. We gratefully acknowledge Drs. Michael W. Extine and B. Frenz for the development of several programs and Dr. Douglas Collins for helpful discussions concerning the treatment of errors.

Registry No. $(CH_3)_2TeCl_2$, 24383-90-2.

Supplementary Material Available: Listing of the root-mean-square amplitudes of thermal vibration, weighted least-squares planes, and the observed and calculated structure factors for both observed and unobserved data (19 pages). Ordering information is given on any current masthead page.

(40) Olovsson, I. In "Electron and Magnetization Densities in Molecules an Crystals"; Becker, P., Ed.; Plenum: New York, 1980; pp 831-894.

(41) Troup, J. M.; Ziolo, R. F., work in progress.

Clusters in Catalysis. High Reactivity in an Electron-Rich Cluster with Weak Metal-Metal Bonds. Facile, Reversible Addition of Carbon Monoxide to $Os_4(CO)_{12}(\mu_3\text{-}S)_2$

Richard D. Adams* and Li-Wu Yang

Contribution from the Department of Chemistry, Yale University, New Haven, Connecticut 06511. *Received March 8, 1982*

Abstract: The cluster complexes $Os_4(CO)_{12}(\mu_3\text{-}S)_2$ (I) and $Os_4(CO)_{13}(\mu_3\text{-}S)_2$ (II) have been synthesized and characterized by IR and mass spectrometry and X-ray crystallographic analyses. For I: space group $P\bar{1}$; a = 8.491 (2) Å, b = 9.240 (2) Å, c = 14.389 (5) Å, α = 80.54 (2)°, β = 85.94 (2)°, γ = 68.31 (5)°, Z = 2, ρ_{calcd} = 3.728 g cm^{-3}. The structure was solved by the heavy-atom method. Least-squares refinement on 2930 reflections ($F^2 \geq 3.0\sigma(F^2)$) produced the final residuals R_1 = 0.032 and R_2 = 0.034. I contains a butterfly cluster of four osmium atoms with sulfido ligands bridging the two open triangular faces and three carbonyl ligands on each metal atom. Electron counting shows that I is a 64-electron cluster, which implies that it should contain only four metal-metal bonds. However, the structural analysis shows the presence of five significant metal-metal interactions. Three of these, at 2.914 (1) Å, 2.935 (1) Å, and 2.940 (1) Å, are close to the normal single bond length of 2.877 (3) Å while the other two are significantly longer at 3.091 (1) Å and 3.002 (1) Å. The relationship of the bonding in this cluster to current theories of cluster bonding is discussed. These longer, weaker metal-metal bonds are very reactive. For example, I absorbs 1 mol of carbon monoxide at 1 atm /25 °C to produce II. For II: space group $P2_1/n$; at 26 °C, a = 10.195 (5) Å, b = 12.679 (4) Å, c = 17.236 (6) Å, β = 96.98 (4)°, Z = 4, ρ_{calcd} = 3.571 g cm^{-3}. The structure was solved by direct methods. Least-squares refinement on 2190 reflections ($F^2 \geq 3.0\sigma(F^2)$) produced the final residuals R_1 = 0.044 and R_2 = 0.043. II contains a planar cluster of four osmium atoms with only three metal-metal bonds. There are 2 triply bridging sulfido ligands and 13 carbonyl ligands (12 linear and 1 semibridge). II can be formed from I by addition of 1 mol of carbon monoxide to one of "hinge" metal atoms followed by complete cleavage of the two weak metal-metal bonds and a shift of a sulfur atom from one hinge metal atom to the other. Surprisingly, the CO addition is fully reversible, such that when heated to reflux in hexane solvent II reverts back to I quantitatively.

Due to their potential as a new class of homogeneous reaction catalysts, transition-metal cluster compounds have attracted considerable attention.[1] Polynuclear coordination[2] and reactions at metal-metal bonds[3] are features that have no parallel at a single

0002-7863/83/1505-0235$01.50/0